International Journal of Engineering Research & Technology (IJERT)
ISSN: 2278-0181
Vol. 6 Issue 05, May - 2017

CDR in Glaucoma Detection using Dissimilarity Constraints Coding

Deepa. D. Raj
PG Scholar
School of CSE
Mar Ephraem College of Engineering and Technology
Elavuvilai, Marthandam, India

Ashwin Singerji
Assistant Professor
School of CSE
Mar Ephraem College of Engineering and Technology
Elavuvilai, Marthandam, India

Shobhana .S
Assistant Professor
School of CSE
Mar Ephraem College of Engineering and Technology
Elavuvilai, Marthandam, India

Anuja Titus
PG Scholar
School of CSE
Mar Ephraem College of Engineering and Technology
Elavuvilai, Marthandam, India

***Abstract*: Glaucoma is an irreversible chronic eye disease that leads to vision loss. As it can be slowed down through treatment, detecting the disease in time is important. However, many patients are unaware of the disease because it progresses slowly without easily noticeable symptoms. Currently, there is no effective method for low cost population-based glaucoma detection or screening. Recent studies have shown that automated optic nerve head assessment from 2D retinal fundus images is promising for low cost glaucoma screening. In this paper, we propose a method for cup to disc ratio (CDR) assessment using 2D retinal fundus images. Methods: In the proposed method, the optic disc is first segmented and reconstructed using a novel sparse dissimilarity-constrained coding (SDC) approach which considers both the dissimilarity constraint and the sparsity constraint from a set of reference discs with known CDRs. Subsequently, the reconstruction coefficients from the SDC are used to compute the CDR for the testing disc. Results: The proposed method has been tested for CDR assessment in a database of 650 images with CDRs manually measured by trained professionals previously. Experimental results show an average CDR error of 0.064 and correlation coefficient of 0.67 compared with the manual CDRs, better than the state-of-the-art methods. Our proposed method has also been tested for glaucoma screening. The method achieves areas under curve of 0.83 and 0.88 on datasets of 650 and 1676 images, respectively, outperforming other methods. Conclusion: The proposed method achieves good accuracy for glaucoma detection. Significance: The method has a great potential to be used for large-scale population-based glaucoma screening.**

Index Terms- Cup to Disc Ratio, Glaucoma Screening, Sparse Dissimilarity-Constrained Coding

I. INTRODUCTION

Glaucoma is a chronic eye disease. It is the leading cause of irreversible blindness, and is predicted to affect around 80 million people by 2020. As the disease progresses silently without easily noticeable visual symptoms especially in the early stages, 50%-90% of patients are unaware of the disease until it has reached its advanced stages. Thus, glaucoma is also called the silent theft of sight. Although glaucoma cannot be cured currently, it can be slowed down through treatment. This makes the screening of people at high risk of glaucoma for timely detection very meaningful. Currently, the air-puff intraocular pressure (IOP) measurement, visual field test and optic nerve head (ONH) assessment are often used in glaucoma assessment. However, the IOP measurement provides low accuracy in glaucoma detection and a visual field examination requires special equipment only present in specialized hospitals. Therefore, they are unsuitable for screening in the population. ONH assessment is more promising for glaucoma screening. It can be done by a trained professional. However, manual assessment is subjective, time consuming and expensive. In recent years, automated algorithms for ONH assessment have received much attention. There is some research into automated CDR assessment from 3D images such as stereo images and optical coherence tomography (OCT) images. However, the cost of obtaining 3D images is still high, which makes it inappropriate for low cost large-scale screening [9]. The 2D retinal fundus images can be acquired at much lower cost because such fundus cameras are widely available in hospitals, polyclinics, eye centers, and especially in optical shops. Therefore, there is little additional hardware cost to build a glaucoma screening programme using existing fundus cameras. This work is for automated CDR assessment from 2D fundus images.

One strategy for automatic ONH assessment is to use image level features for a binary classification between glaucoma-tous and healthy subjects [10], [11], [12]. In these methods, selection of features and classification strategy is difficult and challenging . The other strategy is to follow clinical indicators. Many glaucoma risk factors can be considered, such as the vertical cup to disc ratio (CDR), disc diameter, ISNT rule, etc. Although different ophthalmologists have different opinions on the usefulness of these factors, CDR is well accepted and commonly used. A larger CDR generally indicates a higher risk of glaucoma and vice versa.

International Journal of Engineering Research & Technology (IJERT)
ISSN: 2278-0181
Vol. 6 Issue 05, May - 2017

In 2D retinal fundus images, the ONH or the optic disc can be divided into a central bright zone called the optic cup and a peripheral region called the neuroretinal rim, as shown in Fig. 1. The CDR is computed as the ratio of the vertical cup diameter to the vertical disc diameter clinically. Many methods have been proposed for CDR assessment/computation from 2D images. In thresholding based on intensity is used. However, in many subjects from screening, the cup boundaries are not clear from intensity. Later, relevant vessel bending is used to aid in cup detection [9]. The challenge is to correctly identify the vessel bends. Yin *et al.* developed an active shape model based approach by combining prior knowledge with contour deformation [17]. However, the contour deformation does not work well when the contrast between the cup and rim is weak. Cheng *et al.* proposed superpixel classification based approach [18] by including features from superpixel level, which significantly improves the disc and cup detection. However, it has a bias of under-estimating large cups and over-estimating small cups due to the dominance of medium sized cups used to train the model. Very often, these methods rely on the contrast between the cup and the neuroretinal rim to find the cup boundary for CDR computation and can be challenging to use effectively when the contrast is weak. Recently, Xu *et al.* proposed a reconstruction or atlas based method for cup estimation from the discs [19]. The method applies locality-constrained linear coding (LLC) [20] with _ 2-norm Gaussian distance regularization to reconstruct the disc from a set of reference images with known CDRs. Then it infers the CDR based on the reconstruction coefficients. It significantly reduces the CDR errors. However, the _ 2-norm Gaussian distance suffers from the blood vessels and other noise, which lead to a bias similar to the superpixel based method

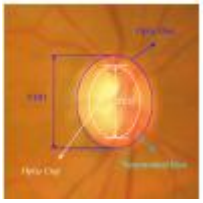

Fig. 1. Structure of an optic disc: optic disc boundary (blue); optic cup (white); neuroretinal rim (cyan); CDR is computed as VCD/VDD.

This paper focuses on computing the CDR from the disc. Motivated from the observation that similar discs often have very similar CDRs and the fact that many discs do not have obvious boundary between neuro-retinal rim and the optic cup, we propose a sparse dissimilarity-constrained coding (SDC) to estimate the CDR for a new disc image. In comparison with the LLC method [19] which uses the Gaussian distance, the proposed method computes the dissimilarities between the testing disc images and the reference disc images from their overall intensity changes and use them as the dissimilarity constraint in the SDC based disc reconstruction. Several major factors that often affect the disc dissimilarity computation and the disc reconstruction have been considered, including blood vessels, uneven illumination within each disc image and the illumination changes between different images. In addition, a sparsity constraint is also included in SDC inspired from the observation that a few reference disc images closest to the testing disc image are usually sufficient to estimate its CDR. The main contributions of this paper include:

1) a novel SDC method for CDR assessment which consid-ers both dissimilarity constraint and sparse constraint;
2) a new method to compute the dissimilarity between two disc images;
3) The results show that the proposed method achieves much more accurate CDR assessment and better glau-coma screening performance than the state-of-the-art methods

Different from most of previous methods which are based on low-level image segmentation, this method computes an optimal sparse linear reconstruction of the input disc from the most similar reference discs to estimate the CDR. This makes the algorithms more robust to the cases where the contrast between optic cup and rim is low.

The rest of the paper is organized as follows. In Section II, we give a brief review of the disc localization and disc segmentation followed by the disc normalization used in this paper. Section III introduces the proposed SDC method for CDR assessment including the computation of disc dissimilar-ity, the formulation of SDC, the solution of SDC, and the CDR assessment using SDC. Section IV shows the experimental results followed by the discussions and conclusions in the last section.

II. DISC LOCALIZATION, SEGMENTATION AND NORMALIZATION

In this paper, we segment the disc using the state-of-the-art self-assessed disc segmentation method [32], which is a combination of three approaches. It has been shown that the self-assessed approach achieves more accurate disc segmentation than the individual methods in [32]. Here we give a brief review of the method while more details can be found in [32].

1) Blood vessel removal: The blood vessels within the disc vary largely among different individuals. The disc recon-struction and the dissimilarity computation between two disc images are greatly affected by them. Therefore, it is important to remove the blood vessels. Many automated vessel detection methods [33][34] reported in the literature can be used. In this application, we found it unnecessary to use very complex and time-consuming vessel segmentation to get precise blood vessels for the disc dissimilarity computation and later the disc reconstruction. Instead, an approximate segmentation of blood vessel is sufficient for the objective of computing the disc dissimilarity. In this paper, we use a morphological closing process with an empirically selected structure element size of 5 to estimate the blood vessels (BV):

$$BV(j,k) = \begin{cases} 1 & \text{If } |x(j,k) - \tilde{x}(j,k)| > T \\ 0 & \text{otherwise} \end{cases}, \quad (1)$$

where $\tilde{x} = morph(x)$ denotes the image after applying a morphological closing process on x. Then, the vessel removed image $\hat{x}$ is obtained by replacing the vessel pixels in x with the pixels in $\tilde{x}$, i.e.,

International Journal of Engineering Research & Technology (IJERT)
ISSN: 2278-0181
Vol. 6 Issue 05, May - 2017

$$\hat{x}(j,k) = \begin{cases} \tilde{x}(j,k) & \text{If } BV(j,k) = 1 \\ x(j,k) & \text{Otherwise} \end{cases} \quad (2)$$

The balance corrected disc x_b is computed as:

$$x_b(j,k) = \frac{(k-k_c)}{k_{max}-p}(\bar{x}_l - \bar{x}_r) + \hat{x}(j,k), \quad (3)$$

III. SPARSE DISSIMILARITY-CONSTRAINED CODING

In this section, we introduce the proposed spare dissimilarity-constrained coding algorithm. Denote a set of *n* reference disc images $X = [x_1, \cdots, x_n]$ and the correspond-ing CDRs as $r = [r_1, r_2, \cdots, r_n]^T$, $i = 1, 2, \cdots, n$, x_i denotes the i^{th} balance corrected disc computed above. Inspired from the reconstruction based method [19], we want to compute a linear reconstruction coefficient $w = [w_1, \cdots, w_n]^T$ for a new testing disc image *y* while minimizing the reconstruction error $\_y - Xw\_^2$. From our experience, a few reference disc images that are closest to *y* are sufficient to estimate the CDR for *y* while too many reference images often lead to a bias especially when the reference images do not have uniform CDR distribution. Therefore, we want to limit the number of reference images used, i.e., we want to minimize the non-zeros elements in *w*, or $\_w\__0$. Because $\__0$-norm is a NP-hard problem, the $\__1$-norm $\_w\__1$ is used instead. In addition, as the reconstruction is more accurate from images more similar to the test disc, we add the difference between the reference and test disc images as a regularization term in the objective function to penalize the use of references. Denoting the difference between *y* and the reference discs in *X* as the vector $d = [d_1, \cdots, d_n]^T$, we want to minimize the overall difference term expressed as $\_d \_ w\_$, where d_i represents the difference between *y* and *xi*, _ denotes the element-wiseproduct. Previously, Gaussian distance $di = \exp(\_y-xi\_2 2\sigma 2)$ between the test disc *y* and the *ith* reference disc *xi* is used in LLC [19]. However, the pixel-wise distance between two disc images suffers from various noise including blood vessels, disc alignment error, etc. In this paper, we propose to compute the dissimilarity between two disc images

A. Dissimilarity

It is important to compute a dissimilarity score between two discs which reflects their CDR difference. As mentioned, the previously used Gaussian distance [19] often suffers from noise, imperfect vessel removal etc. Therefore, it faces some challenges to represent the actual CDR difference between two discs. Very often, we found two discs with similar CDRs have a Gaussian distance even larger than two discs with significant different CDRs. Therefore, Gaussian distance is not a good choice. In fact, this is also the reason that a k nearest neighbor (kNN) approach works poorly for this task. In this paper, we observe that the overall intensity change within the disc is highly related with the CDR value. Motivated from this, we propose to apply surface fitting within the disc image to compute the dissimilarity. Fig. 3 shows an example of a disc image plotted in 3D and its best fitted surface. Although higher order polynomials can be computed, a second order two-dimensional polynomial surface S(j, k) is sufficient to capture the overall intensity change by $\vec{v} = [a, b, c, e, g]^T \in \mathbb{R}^5$:

$$S(j,k) = aj^2 + bj + ck^2 + ek + g = (\vec{q})^T \cdot \vec{v} \quad (4)$$

Where $\vec{q} = [j^2, j, k^2, k, 1]^T$ and T denotes the transpose. This can be expressed in matrix form as

$$\vec{s} = Q\vec{v} \quad (5)$$

where s contains the coefficients S(j, k) strung out into a column vector, and the matrix Q contains the coefficients of q as specified in Equation (4). The coefficient v is then determined by minimizing the following quadratic error between s and x, where x contains the intensities of the disc image xi or y strung out into a column vector

$$\begin{aligned} E(\vec{v}) &= (\vec{x} - \vec{s})^2 \\ &= (\vec{x} - Q\vec{v})^2 \end{aligned} \quad (6)$$

As the blood vessels are not relevant to the overall intensity changes of the discs, we exclude pixels belonging to blood vessels extracted previously, i.e., pixels (j, k) with BV (j, k) It can be seen that

$$\vec{v} = (Q^T Q)^{-1} Q^T \vec{x} \quad (7)$$

The difference between two surfaces Sxi and Sy is computed from their coefficients vxi and vy. As the overall intensity change of the disc is only related to the a and c components axi , cxi , ay, cy, the difference di between the two surfaces can be computed by a function f(axi , cxi , ay, cy). Here, the subscript denotes the disc used to compute the surface parameters. In this paper, we use

$$d_i = f(a_{x_i}, c_{x_i}, a_y, c_y) = \sqrt{(a_{x_i} - a_y)^2 + (c_{x_i} - c_y)^2} \quad (8)$$

B. Formulation of sparse dissimilarity-constrained coding

The objective function of the proposed SDC method is then given by:

$$\underset{w}{\operatorname{argmin}} \|y - Xw\|^2 + \lambda_1 \cdot \|d \odot w\|^2 + \lambda_2 \cdot \|w\|_1, \quad (9)$$

where λ1 and λ2 are parameters controlling the weights of the two regularization items. Rewriting the second item and merging it with the first item in (9), we get

$$\begin{aligned} &\underset{w}{\operatorname{argmin}} \left(\|y - Xw\|^2 + \lambda_1 \cdot \|d \odot w\|^2 + \lambda_2 \cdot \|w\|_1\right) \\ = &\underset{w}{\operatorname{argmin}} \left(\|y - Xw\|^2 + \lambda_1 \cdot \|Dw\|^2 + \lambda_2 \cdot \|w\|_1\right) \\ = &\underset{w}{\operatorname{argmin}} \left(\left\| \begin{bmatrix} y \\ \mathbf{0} \end{bmatrix} - \begin{bmatrix} X \\ \sqrt{\lambda_1} D \end{bmatrix} w \right\|^2 + \lambda_2 \cdot \|w\|_1\right) \\ = &\underset{w}{\operatorname{argmin}} \left(\|\hat{y} - \hat{X}w\|^2 + \lambda_2 \cdot \|w\|_1\right) \end{aligned} \quad (10)$$

C. Solution

The problem in (10) is a standard _1 norm regularized least square minimization problem. It has been shown that this unconstrained convex optimization problem can be representedas the following constrained optimization problem [35]:

$$\underset{w}{\operatorname{argmin}} \left(\|\hat{y} - \hat{X}w\|^2\right), s.t., \|w\|_1 < t, \quad (11)$$

International Journal of Engineering Research & Technology (IJERT)
ISSN: 2278-0181
Vol. 6 Issue 05, May - 2017

where t is inversely related to λ2. It can be solved by least angle regression (LARS) [36].

V. EXPERIMENTAL RESULTS

A. Data set and Evaluation Criteria

In this paper, we use these manual CDRs as'ground truth' unless specified. The SCES images are collected in a screening study. There are two sizes: 3504 × 2336 and3888×2592. All the SCES images are resized to be the same size as the SiMES set for convenience. Among the 2326 eyes,168 SiMES and 46 SCES eyes are diagnosed as glaucomatous by ophthalmologists. These diagnostic outcomes are used asthe gold ground truth. The disc localization method in [23]
is used to locate the disc and determine an 800 × 800 region of interest for disc segmentation. It locates the disc correctly in all 650 SiMES images. In SCES, it fails in four of 1676 images.

B. Comparison with other methods

TABLE I
PERFORMANCE BY VARIOUS METHODS.

	CDR Error	Pearson Correlation	AUC	
			SiMES	SCES
Airpuff IOP	-	-	0.59	0.66
Superpixel [18]	0.078	0.59	0.80	0.82
LLE [39]	0.080	0.47	0.75	0.74
SC [38]	0.071	0.59	0.80	0.85
LLC [19]	0.072	0.60	0.81	0.86
Proposed	0.064	0.67	0.83	0.88
Expert B	0.078	0.63	0.82	-
Expert A	-	-	0.84	-

TABLE I
PERFORMANCE BY VARIOUS METHODS.

	CDR Error	Pearson Correlation	AUC	
			SiMES	SCES
Airpuff IOP	-	-	0.59	0.66
Superpixel [18]	0.078	0.59	0.80	0.82
LLE [39]	0.080	0.47	0.75	0.74
SC [38]	0.071	0.59	0.80	0.85
LLC [19]	0.072	0.60	0.81	0.86
Proposed	0.064	0.67	0.83	0.88
Expert B	0.078	0.63	0.82	-
Expert A	-	-	0.84	-

IV. CONCLUSION

The proposed SDC method achieves CDR computation and glaucoma detection accuracy comparable with manual CDR assessment by experts. It suggests that the proposed method can be used to replace the time-consuming and expensive manual CDR assessment. Therefore, the proposed method has great potential for low cost glaucoma screening in polyclinics, eye centers, and especially in optical shops, according to discussions with clinicians and ophthalmologists. This paper discussed the proposed SDC for CDR computation within this paper, the general formulation in (9) can be extended for other applications, though the computation of the *d* might need to be specially defined based on actual data. The CDR based screening from 2D images has its limitations. For example, 2D images do not have depth information, which is the primary indicator of cup. Compared with 3D images which capture true 3D morphological structures of disc and cup, 2D images capture the color information of disc and rely on intensities to estimate the CDR. Future work will explore the integration of other factors to improve diagnostic outcomes towards a more reliable and efficient glaucoma screening system.

REFERENCES

[1] H. A. Quigley and A. T. Broman, "The number of people with glaucoma worldwide in 2010 and 2020," *Br. J. Ophthalmol.*, vol. 90(3), pp. 262– 267, 2006.

[2] S. Y. Shen, T. Y. Wong, P. J. Foster, J. L. Loo, M. Rosman, S. C. Loon, W. L. Wong, S. M. Saw, and T. Aung, "The prevalence and types of glaucoma in malay people: the singapore malay eye study," *Invest. Ophthalmol. Vis. Sci.*, vol. 49(9), pp. 3846–3851, 2008.

[3] P. J. Foster, F. T. Oen, D. Machin, T. P. Ng, J. G. Devereux, G. J. Johnson, P. T. Khaw, and S. K. Seah, "The prevalence of glaucoma in chinese residents of singapore: a cross-sectional population survey of the tanjong pagar district," *Arch. Ophthalmol.*, vol. 118(8), pp. 1105–1111, 2000.

[4] Centre for Eye Research Australia, *Tunnel vision : the economic impact of primary open angle glaucoma. [electronic resource]*, 2008, http://nla.gov.au/nla.arc-86954.

[5] M. D. Abr`amoff, W. L. M. Alward, E. C. Greenlee, L. Shuba, C. Y. Kim, J. H. Fingert, and Y. H. Kwon, "Automated segmentation of theoptic disc from stereo color photographs using physiologically plausible features," *Invest. Ophthalmol. Vis. Sci.*, vol. 48, pp. 1665–1673, 2007.

[6] J. Xu, O. Chutatape, E. Sung, C. Zheng, and P.C.T. Kuan, "Optic disk feature extraction via modified deformable model technique for glaucoma analysis," *Pattern Recognition*, vol. 40, pp. 2063–2076, 2007.

[7] Z. Hu, M. D. Abr`amoff, Y. H. Kwon, K. Lee, and M. K. Garvin,"Automated segmentation of neural canal opening and optic cup in 3-d spectral optical coherence tomography volumes of the optic nerve head," *Inv Ophthalmol Vis Sci.*, vol. 51, pp. 5708–5717, 2010.

[8] M. D. Abr`amoff, K. Lee, M. Niemeijer, W. L. M. Alward, E. Greenlee, M. K. Garvin, M. Sonka, and Y. H. Kwon, "Automated segmentation of the cup and rim from spectral domain oct of the optic nerve head," *Inv Ophthalmol Vis Sci.*, vol. 50, pp. 5778–5784, 2009.

[9] G. D. Joshi, J. Sivaswamy, and S. R. Krishnadas, "Optic disk and cup segmentation from monocular color retinal images for glaucoma assessment," *IEEE Trans. Med. Imag.*, vol. 30, pp. 1192–1205, 2011.

[10] J. Meier, R. Bock, G. Michelson, L. G. Nyl, and J. Hornegger, "Effects of preprocessing eye fundus images on appearance based glaucoma classification," *Proc. CAIP*, pp. 165–172, 2007.

[11] R. Bock, J. Meier, G.Michelson, L. G. Nyl, and J. Hornegger, "Classifying glaucoma with image-based features from fundus photographs," *Proc. of DAGM*, pp. 355–364, 2007.

[12] R. Bock, J. Meier, L. G. Nyl, and G. Michelson, "Glaucoma risk index: Automated glaucoma detection from color fundus images," *Med. Image Anal.*, vol. 14, pp. 471–481, 2010.

[13] T. Damms and F. Dannheim, "Sensitivity and specificity of optic disc parameters in chronic glaucoma," *Invest. Ophth. Vis. Sci.*, vol. 34, pp. 2246–2250, 1993.

[14] D. Michael and O. D. Hancox, "Optic disc size, an important consideration in the glaucoma evaluation," *Clinical Eye and Vision Care*, vol. 11, pp. 59–62, 1999.

International Journal of Engineering Research & Technology (IJERT)
ISSN: 2278-0181
Vol. 6 Issue 05, May - 2017

[15] N. Harizman, C. Oliveira, A. Chiang, C. Tello, M. Marmor, R. Ritch, and JM. Liebmann, "The isnt rule and differentiation of normal from glaucomatous eyes," vol. 124, pp. 1579–1583, 2006.

[16] G. D. Joshi, J. Sivaswamy, K. Karan, and R. Krishnadas, "Optic disk and cup boundary detection using regional information," *in Proc. IEEE Int. Symp. Biomed. Imag.*, pp. 948–951, 2010.

[17] F. Yin, J. Liu, D. W. K. Wong, N. M. Tan, C. Cheung, M. Baskaran, T. Aung, and T. Y. Wong, "Automated segmentation of optic disc and optic cup in fundus images for glaucoma diagnosis," *IEEE Int. Symp. on Computer-Based Medical Systems*, pp. 1–6, 2012.

[18] J. Cheng, J. Liu, Y. Xu, F. Yin, D. W. K. Wong, N. M. Tan, D. Tao, C. Y. Cheng, T. Aung, and T. Y. Wong, "Superpixel classification based optic disc and optic cup segmentation for glaucoma screening," *IEEE Trans. Med. Imaging*, vol. 32, pp. 1019–1032, 2013.

[19] Y. Xu, S. Lin, D. W. K. Wong, J. Liu, and D. Xu, "Efficient reconstruction-based optic cup localization for glaucoma screening," *In: Mori, K., Sakuma, I., Sato, Y., Barillot, C., Nassir, N.(eds.) MICCAI 2013, Part III, LNCS*, vol. 8151, pp. 445–452, 2013.

[20] J. Wang, J. Yang, K. Yu, F. Lv, T. Huang, and Y. Gong, "Localityconstrained linear coding for image classification," *IEEE Int. Conf. on computer vision and pattern recognition*, pp. 3360–3367, 2010.

[21] M. D. Abr`amoff, M. K. Garvin, and M. Sonka, "Retinal imaging and image analysis," *IEEE Trans. Med. Imag.*, vol. 3, pp. 169–208, 2010.

[22] H. Li and O. Chutatape, "Automatic location of optic disc in retinal images," *in Proc. Int. Conf. Image Processing*, vol. 2, pp. 837–840, 2001.

[23] Z. Zhang, B. H. Lee, J. Liu, D. W. K. Wong, N. M. TAN, J. H. Lim, F. S. Yin, W. M. Huang, and H. Li, "Optic disc region of interest localization in fundus image for glaucoma detection in argali," *Proc. of Int. Conf. on Industrial Electronics & Applications*, pp. 1686–1689, 2010.

[24] A. Hoover and M. Goldbaum, "Locating the optic nerve in a retinal image using the fuzzy convergence of the blood vessels," *IEEE Trans. Med. Imag.*, vol. 22, pp. 951–958, 2003.

[25] M. Foracchia, E. Grisan, and A. Ruggeri, "Detection of optic disc in retinal images by means of a geometrical model of vessel structure," *IEEE Trans. Med. Imag.*, vol. 23, no. 10, pp. 1189–1195, 2004.

[26] H. Li and O. Chutatape, "Automated feature extraction in color retinal images by a model based approach," *IEEE Trans. Biomed. Eng.*, vol. 51, no. 2, pp. 246–254, Feb 2004.

[27] A. P. Rovira and E. Trucco, "Robust optic disc location via combination of weak detectors," *in Proc. Int. Conf. IEEE Eng. Med. Bio. Soc.*, pp. 3542–3545, 2008.

[28] A. Aquino, M. Gegundez-Arias, and D. Marin, "Detecting the optic disc boundary in digital fundus images using morphological, edge detection, and feature extraction techniques," *IEEE Trans. Med. Imag.*, vol. 29, pp. 1860–1869, 2010.

[29] J. Cheng, J. Liu, D. W. K. Wong, F. Yin, C. Cheung, M. Baskaran, T. Aung, and T. Y. Wong, "Automatic optic disc segmentation with peripapillary atrophy elimination," *Int. Conf. of IEEE Eng. in Med. And Bio. Soc.*, pp. 6624–6627, 2011.

[30] F. Yin, J. Liu, S. H. Ong, Y. Sun, D. W. K. Wong, N. M. Tan, C. heung, M. Baskaran, T. Aung, and T. Y. Wong, "Model-based optic nerve head segmentation on retinal fundus images," *Int. Conf. of IEEE Eng. in Med. and Bio. Soc.*, pp. 2626–2629, 2011.

[31] J. Cheng, J. Liu, Y. Xu, F. Yin, D. W. K. Wong, N. M. Tan, C. Y. Cheung, Y. C. Tham, and T. Y. Wong, "Superpixel classification based optic disc segmentation," *In: Lee, K. M., Matsushita, Y., Rehg, J. M., Hu, Z. (eds.) ACCV, Part II, LNCS*, vol. 7725, pp. 293–304, 2013.

[32] J. Cheng, J. Liu, F. Yin, B. H. Lee, D. W. K. Wong, T. Aung, C. Y. Cheng, and T. Y. Wong, "Self-assessment for optic disc segmentation," *IEEE Int. Conf. Eng. in Med. and Bio. Soc.*, pp. 5861–5864, 2013.

[33] T. Chanwimaluang and G. Fan, "An efficient blood vessel detection algorithm for retinal images using local entropy thresholding," vol. 5, pp. 21–24, 2003.

[34] C. A. Lupascu, D. Tegolo, and E. Trucco, "Fabc: Retinal vessel segmentation using adaboost," *IEEE Trans. on Information Technology in Biomedicine*, vol. 14, no. 5, pp. 1267–1274, 2010.

[35] M. Schmidt, "Lease squares optimization with l1-norm regularization," *Technical report, University of British Columbia*, 2005.

[36] B. Efron, T. Hastie, and R. Tibshirani, "Least angle regression," *Annals of Statistics*, vol. 32, pp. 68–73, 2004.

[37] Z. Zhang, F. Yin, J. Liu, W. K. Wong, N. M. Tan, B. H. Lee, J. Cheng, and T. Y. Wong, "Origa-light: An online retinal fundus image database for glaucoma analysis and research," *Int. Conf. of IEEE Eng. in Med and Bio. Soc.*, pp. 3065–3068, 2010.

[38] B. A. Olshausen and D. J. Field, "Emergence of simple-cell receptive field properties by learning a sparse code for natural images," *Nature*, vol. 381(6583), pp. 607–609, 1996.

[39] S. Roweis and L. Saul, "Nonlinear dimensionality reduction by locally linear embedding," *Science*, vol. 290(5500), pp. 2323–2326, 2000.